Genetic Control of Splicing at *SIRPG* Modulates Risk of Type 1 Diabetes

Morgan J. Smith,[1,2] Lucia Pastor,[2,3] Jeremy R.B. Newman,[2,3] and Patrick Concannon[2,3]

Diabetes 2022;71:350–358 | https://doi.org/10.2337/db21-0194

Signal regulatory protein SIRPγ (CD172G) is expressed on the surface of lymphocytes, where it acts by engaging its ligand, CD47. *SIRPG,* which encodes SIRPγ, contains a nonsynonymous coding variant, rs6043409, which is significantly associated with risk for type 1 diabetes. *SIRPG* produces multiple transcript isoforms via alternative splicing, all encoding potentially functional proteins. We show that rs6043409 alters a predicted exonic splicing enhancer, resulting in significant shifts in the distribution of *SIRPG* transcript isoforms. All of these transcript isoforms produced protein upon transient expression in vitro. However, CRISPR/Cas9 targeting of one of the alternatively spliced exons in *SIRPG* eliminated all SIRPγ expression in Jurkat T cells. These targeted cells formed fewer cell-cell conjugates with each other than with wild-type Jurkat cells, expressed reduced levels of genes associated with CD47 signaling, and had significantly increased levels of cell-surface CD47. In primary CD4$^+$ and CD8$^+$ T cells, cell-surface SIRPγ levels in response to anti-CD3 stimulation varied quantitatively by rs6043409 genotype. Our results suggest that *SIRPG* is the most likely causative gene for type 1 diabetes risk in the 20p13 region and highlight the role of alternative splicing in lymphocytes in mediating the genetic risk for autoimmunity.

The signal regulatory protein (SIRP) family of receptor proteins is encoded by a cluster of five genes at chromosome 20p13. The archetypal member of this gene family, *SIRPA*, encodes SIRPα (CD172A), a receptor expressed on myeloid and neuronal cells that transduces inhibitory signals upon binding CD47 or surfactant proteins (1). SIRPγ, encoded by *SIRPG*, also binds CD47 but with 10-fold lower affinity than SIRPα and has only a four–amino acid cytoplasmic tail lacking any residues or motifs that might facilitate intracellular signaling (2). Uniquely among SIRP family members, SIRPγ is expressed on lymphocytes, specifically T cells, activated natural killer (NK) cells, and a small subset of CD19$^+$ B cells. While SIRPγ is lacking in any apparent capability of signaling intracellularly, SIRPγ engagement by CD47 has been implicated in cell-cell adhesion, proliferation in response to superantigen stimulation, apoptosis, and *trans*-endothelial migration of T cells (2–4).

Genome-wide association studies originally identified the chromosome 20p13 region in humans as harboring a risk locus for type 1 diabetes (5) (Supplementary Fig. 1). Fine mapping further refined this association, identifying a credible causative variant, rs6043409, a G-to-A substitution that results in the replacement of alanine with valine at position 263 in exon 4 of SIRPγ (6). The minor allele of rs6043409 (A) is associated with reduced risk for type 1 diabetes ($P = 3.9 \times 10^{-10}$; odds ratio 0.87) (7). However, the amino acid substitution encoded by rs6043409 is conservative, the mechanism whereby this variant might affect risk for type 1 diabetes is unknown, and the function of SIRPγ is poorly understood. It has been reported that the level of cell-surface expression of SIRPγ on CD8$^+$ T cells varies with genotype at another, noncoding variant in the region, rs2281808 (8), whose alleles are correlated with those at rs6043409 ($r^2 = 0.89$).

In a prior study of lymphocyte transcriptomes, we observed that genes associated with risk for autoimmunity in general, and type 1 diabetes, specifically, were significantly enriched for alternative splicing events (9). Multiple alternatively spliced *SIRPG* transcripts have been

[1]Biomedical Sciences Training Program, University of Florida College of Medicine, Gainesville, FL
[2]University of Florida Genetics Institute, Gainesville, FL
[3]Department of Pathology, Immunology and Laboratory Medicine, University of Florida College of Medicine, Gainesville, FL

Corresponding author: Patrick Concannon, patcon@ufl.edu

Received 5 March 2021 and accepted 15 November 2021

This article contains supplementary material online at https://doi.org/10.2337/figshare.17026610.

identified: the canonical transcript isoform 1, which uses all six exons; isoform 2, which uses alternative transcriptional and translational start sites; and isoforms 3 and 4, which differ in their inclusion or exclusion of exons 3 and 4 (Supplementary Fig. 2). Here, we demonstrate that risk for type 1 diabetes encoded in the 20p13 chromosomal region is modulated through shifts in the distribution of *SIRPG* transcript isoforms as a consequence of disruption of a predicted exonic splicing enhancer by rs6043409. This results in differential cell-surface expression of SIRPγ on both $CD4^+$ and $CD8^+$ T cells. We further show that variation in SIRPγ expression affects cell-cell adhesion, gene expression, and cell-surface CD47 levels.

RESEARCH DESIGN AND METHODS

Human Subjects

Genomic DNA and viably frozen peripheral blood mononuclear cells (PBMCs) were provided by the Type 1 Diabetes Genetics Consortium (T1DGC). PBMC samples were obtained from individuals of European ancestry ages 35–50 years and collected in North America. All samples had been genotyped previously with the Immunochip, a custom Illumina genotyping array (6). Use of these samples and data was approved by the University of Florida Institutional Review Board.

Cell Isolation and Expansion

$CD4^+$ T cells were isolated with the $CD4^+$ T Cell Isolation Kit, human (Miltenyi Biotec), following the protocol provided by the manufacturer. $CD4^+$ cells were activated and expanded with Dynabeads (Thermo Fisher Scientific) according to instructions provided by the manufacturer.

RNA Extraction and cDNA Preparation

RNA was isolated from $CD4^+$ T cells with the RNeasy Plus Mini Kit (QIAGEN). RNA quantity and purity were assessed by spectrophotometry. RNA was reverse transcribed with iScript reverse transcriptase and oligo(dT) primers (Bio-Rad Laboratories).

Expression of SIRPG Isoforms

$CD4^+$ T cell cDNA for *SIRPG* transcript isoforms was tested in quadruplicate by real-time quantitative PCR with TaqMan Gene Expression Probes. Samples were normalized to two reference probes, *RPL13A* and *IPO8*, and relative expression was analyzed with use of the efficiency correction method (10).

Vectors for the expression of *SIRPG* isoforms were prepared in pEF-DEST51 (12285011; Invitrogen) and confirmed by sequencing. *SIRPG* expression vectors were transfected into HEK293T cells with the X-tremeGENE HP DNA Transfection Reagent (Roche). Cells were harvested 48 h posttransfection for protein analyses.

RNA-Sequencing Analysis

Methods for quality control, alignment, and normalization of RNA-sequencing (RNA-seq) data have previously been previously (9). The data sets analyzed include existing RNA-seq data from $CD4^+$ T cells, $CD8^+$ T cells, and $CD19^+$ B cells from 82 individuals established as having type 1 diabetes as well as newly generated RNA-seq data from Jurkat cell clones derived from CRISPR/Cas9 targeting experiments (five *SIRPG* exon 4–targeted clones, four wild-type clones). For samples passing quality control, paired-end sequencing reads were aligned to human Ensembl (11) transcript sequences with RSEM (12) (version 1.2.28) with default settings. References for RSEM were prepared with "rsem-prepare-reference" and transcript sequences for the complete Ensembl transcriptome (release 99) derived from the GRCh38/hg38 reference genome and a tab delimited gene-to-transcript index file, as previously described (9). Estimates of transcript expression were expressed as transcripts per million and log transformed.

Immunoblotting

Protein from whole cell lysates was separated on Bolt 4–12% Bis-Tris Plus gels (Invitrogen). Protein was transferred to a polyvinyladene difluoride membrane (IPVH20200; Immobilon) with use of the Novex XCell II Blot Module (Life Technologies). Antibodies to SIRPγ (1:2,000; Sigma-Alrich), V5 (1:5,000; Invitrogen), γ-tubulin (1:10,000; Sigma-Aldrich), and GAPDH (1:1,000; Santa Cruz Biotechnology) were used in immunoblotting. $CD4^+$ T cell SIRPγ signal was normalized to the GAPDH loading control following densitometric analyses with ImageQuant TL v8.1.0.0 software.

Gene Editing and Clone Selection

With use of transcript ENST00000303415.7 as a reference, we targeted exon 4 in Jurkat-p2 cells using a single-guide RNA with the sequence GGUGAACAUAUCUGACCAAA. Cloned Jurkat lines were isolated through serial dilution in U-bottom 96-well plates. Clones containing truncating mutations were identified by genomic DNA extraction, PCR amplification, and Sanger DNA sequencing.

Characterization of *SIRPG*-Targeted Clones by Flow Cytometry

SIRPG-targeted clones were expanded in supplemented RPMI medium, and SIRPγ expression was analyzed by flow cytometry. To avoid antibody competition, SIRPγ surface and intracellular staining was performed in separate test wells with the same antibody. After washing twice in PBS, cells were resuspended in PBS–1% FBS at a density of 1 million/tube and stained for viability with the LIVE/DEAD Fixable Near-IR Dead Cell Stain Kit (Thermo Fisher Scientific) for 30 min according to the manufacturer's protocol. After washing twice in PBS–1% FBS, cells were incubated in a U-bottom 96-well plate with anti-SIRPγ antibody (BV421 Mouse Anti-Human SIRPγ Clone OX-119, BD Biosciences, or PE anti-human

CD172g [SIRPγ] Clone LSB2.20, BioLegend) or corresponding isotype control for either 20 min for surface staining or 30 min for intracellular staining with use of Brilliant Stain Buffer (BD Biosciences) and eBioscience Intracellular Fixation & Permeabilization Buffer Set (Thermo Fisher Scientific). Cells were acquired in a BD LSRFortessa cytometer (BD Biosciences) and analyzed with FlowJo software (FlowJo 10.7.1) according to the gating strategy described in Supplementary Fig. 6.

For the analysis of CD47 surface expression, *SIRPG*-targeted clones were labeled with anti-CD47 antibody (PE Mouse Anti-Human CD47 Clone B6H1 [RUO]; BD Biosciences) or a corresponding isotype control following the manufacturer's instructions as described above. Cells were acquired in a BD LSRFortessa cytometer and analyzed for CD47 bright cell expression (expression $>10^4$) after selection for no debris, morphology, and singlets.

Cell Conjugation Assay

Doublet formation was assayed as described by Piccio et al. (3). Briefly, Jurkat cell clones were labeled with distinguishable cell-permeable dyes, Vybrant DiO and DiD (V-22886 and V-22887, respectively; Molecular Probes). Various combinations of cells (2×10^5 of each) were mixed, centrifuged, and incubated at 37°C for 30 min. Conjugates were gently resuspended in a small volume of medium for flow cytometric analysis on BD LSRFortessa cytometer. Cells that had fused or formed stable clusters were identified through double labeling.

Population Testing of SIRPγ Expression

PBMCs were thawed and resuspended in FACS buffer (PBS without calcium and magnesium, 5 mg/mL BSA, 0.1% NaN_3), blocked with TruStain FcX (BioLegend), and stained with directly conjugated antibodies according to standard procedures for cell-surface staining. Antibodies to SIRPγ (BioLegend), CD4 (BioLegend), and CD8 (560179; BD Biosciences) were used. A 7-AAD viability stain (BioLegend) was also applied. Analysis was performed with the BD Accuri C6 (BD Biosciences) and FlowJo 10.0.8r1 software.

Statistical Analysis

Statistical analyses were conducted in Prism software (version 7.03). Hypotheses were evaluated with the Kruskal-Wallis test or Mann-Whitney *U* test. A significance level of 0.05 was defined, and Bonferroni correction was applied where appropriate.

Data and Resource Availability

The RNA-seq data set analyzed in the current study is available from dbGaP (https://www.ncbi.nlm.nih.gov/gap) under accession no. phs001426.v1.p1. Genotypes at rs6043409 for all of these individuals with RNA-seq data are also available in dbGaP under accession no. phs000911.v1.p1.

RESULTS

SIRPG Transcript Isoform Prevalence Is Conditional on Genotype at rs6043409

The rs6043409 variant encodes a conservative Ala-to-Val amino acid substitution in exon 4 of *SIRPG*. Neither computational predictions by SIFT (13) or PolyPhen-2 (14) nor molecular modeling using Phyre2 (15) provided evidence that this substitution would significantly impact SIRPγ protein structure or function. However, an analysis with the program ESEfinder (16) predicted that the minor allele at rs6043409 would disrupt an exonic splicing enhancer by eliminating a predicted binding site for SRSF1, a splicing factor that is highly expressed in lymphocytes. Multiple transcript isoforms of *SIRPG*, generated by the inclusion or exclusion of exons 3 and 4, have been reported (www.ncbi.nlm.nih.gov/IEB/Research/Acembly) (11) (Supplementary Fig. 2). Each of these exons encodes a complete immunoglobulin homology unit. Their inclusion or exclusion does not alter the reading frame of the protein but could have structural or functional consequences for SIRPγ.

$CD4^+$ T cells from each of 24 unaffected subjects representing different rs6043409 genotypes were expanded in vitro, and both RNA and protein were isolated. Quantitative PCR assays were carried out with fluorescently labeled probes specific for *SIRPG* transcript isoforms 1 and 2, isoform 3, or isoform 4 as well as a probe detecting all isoforms. *SIRPG* isoforms 1 and 2 exhibited a statistically significant reduction in expression in subjects homozygous for the minor A allele as compared with those homozygous for the major G allele ($P = 0.003$) (Fig. 1*A*). Isoform 3 displayed the opposite trend, although differences between genotypes for the expression of this isoform were not statistically significant.

To extend these isoform-specific findings to larger numbers of subjects and explore their disease relevance, we examined *SIRPG* expression in RNA-seq data from $CD4^+$ and $CD8^+$ T cells obtained from 82 unrelated subjects with type 1 diabetes (9). We counted reads that mapped uniquely to specific *SIRPG* transcript isoforms, an approach termed Event Analysis (17). By counting events, it is possible to resolve each of the four *SIRPG* transcript isoforms and to compare their relative abundance. Expression of the alternative first exon unique to *SIRPG* transcript isoform 2 showed little or no evidence of expression, whereas isoforms 1, 3, and 4 were predicted as all exons that comprise these transcripts were detected. We then compared the estimated expression of each isoform between rs6043409 genotypes (Fig. 1*B*). Statistically significant differences in abundance by genotype were observed for *SIRPG* transcript isoforms 1 and 3 in both $CD4^+$ and $CD8^+$ T cells. The predominant transcript isoform encoding SIRPγ, in subjects with type 1 diabetes, was dependent on their genotype at rs6043409. Isoforms 2 and 4 did not vary significantly in abundance by genotype

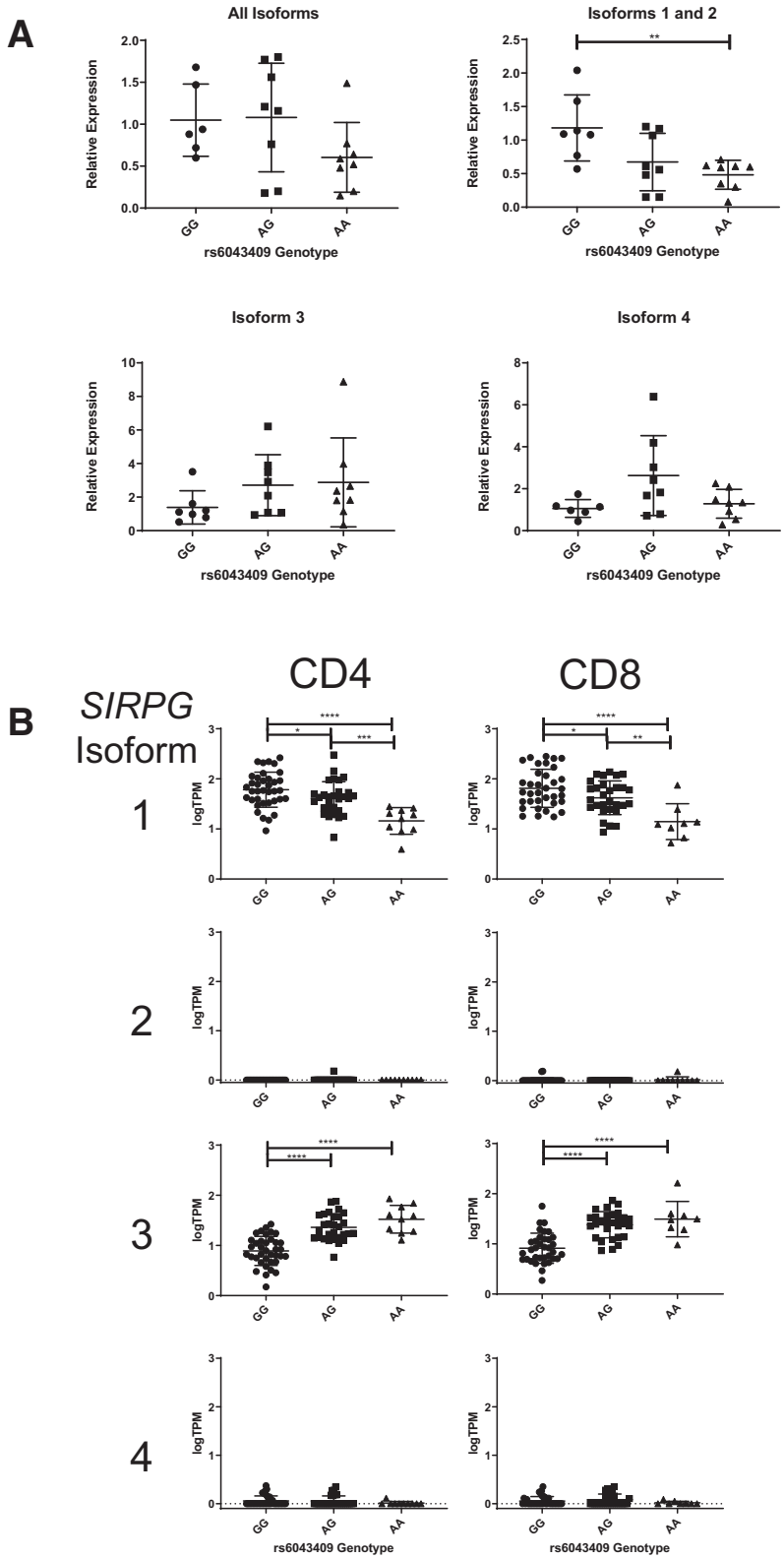

Figure 1—*SIRPG* transcript isoforms and their expression in T cells. *A*: Relative expression of *SIRPG* transcript isoforms in $CD4^+$ T cells from control individuals of different genotypes at rs6043409, as determined by quantitative PCR, is shown. Vertical lines and bars indicate the mean value ± 1 SD. $^{**}P$ value < 0.01. *B*: The log of transcripts per million (TPM) in $CD4^+$ and $CD8^+$ T cells is plotted separately for each *SIRPG* isoform relative to the genotype of the donor at rs6043409. Scales of the vertical axes are the same for all graphs, so the relative expression of different isoforms, as well as differences by genotype, can be compared. Vertical lines and bars indicate the mean value ± 1 SD. Statistically significant comparisons are indicated as follows: $^{*}P < 0.05$, $^{**}P < 0.01$, $^{***}P < 0.001$, and $^{****}P < 0.0001$.

but accounted for only 0.74–5.47% of total *SIRPG* transcripts (Fig. 1*B* and Supplementary Fig. 3).

SIRPG Transcripts Differ in Their Ability to Produce SIRPγ Protein

To determine whether all four detected *SIRPG* transcript isoforms produced corresponding protein isoforms, we immunoblotted for SIRPγ using increasing amounts of protein lysate from Jurkat T cells and a B lymphoblastoid cell line, Sweig (Fig. 2*A*). Proteins corresponding approximately to the predicted molecular weights of isoforms 1 (42 kDa), 2 (38 kDa), and 4 (30 kDa) were detectable at all protein concentrations in Jurkat cells. No protein product corresponding to the predicted molecular weight of isoform 3 (18 kDa) was detected

To evaluate the ability of each transcript isoform to produce a stable protein, the individual isoforms were cloned into expression vectors with a carboxy-terminal V5 epitope tag and transiently transfected into HEK293T cells, and total cellular protein was isolated. Probing immunoblots prepared from these transfected cells with an antibody directed against the V5 epitope tag revealed bands consistent with the production of protein by each of the four transcript isoforms (Fig. 2*B*). This suggests that the failure to detect an endogenously expressed protein product corresponding to isoform 3 in Jurkat cells was not due to an intrinsic instability in this SIRPγ isoform. Additional bands with molecular weights slightly greater than predicted for isoforms 1 and 4 were also detected. Treatment of lysates with the endoglycosidase PNGaseF eliminated these higher–molecular weight bands, indicating that they most likely represent glycosylated forms of SIRPγ (Supplementary Fig. 4).

SIRPG transcript isoform 3 is expressed at significantly higher levels in subjects carrying at least one copy of the minor (A) allele at rs6043409. Thus, the failure to detect a protein corresponding to this transcript isoform could be due to the fact that Jurkat cells are homozygous for the major (G) allele at rs6043409 (18). Whole cell lysates were prepared from $CD4^+$ T cells purified from subjects with different genotypes at rs6043409 and immunoblotted for SIRPγ (Fig. 2*C*). No evidence of a protein corresponding to *SIRPG* transcript isoform 3 was detected despite the use of an antibody targeting a conserved sequence present in all *SIRPG* isoforms.

Cell-Surface and Intracellular Expression of SIRPγ Isoforms

We used CRISPR/Cas9 technology to generate cloned lines of Jurkat cells with truncating mutations in exon 4 of *SIRPG* (Supplementary Table 1). Exon 4 is included in isoforms 1 and 2 but absent from isoforms 3 and 4 (Supplementary Fig. 2). Cell-surface and intracellular levels of SIRPγ expression in clones with either monoallelic or biallelic truncating mutations in *SIRPG* were quantified by flow cytometry. In clones with biallelic truncating mutations in *SIRPG* exon 4, where only proteins corresponding to isoforms 3 and 4 could be expressed, SIRPγ cell-surface expression was undetectable and intracellular expression of SIRPγ was negligible. However, in clones

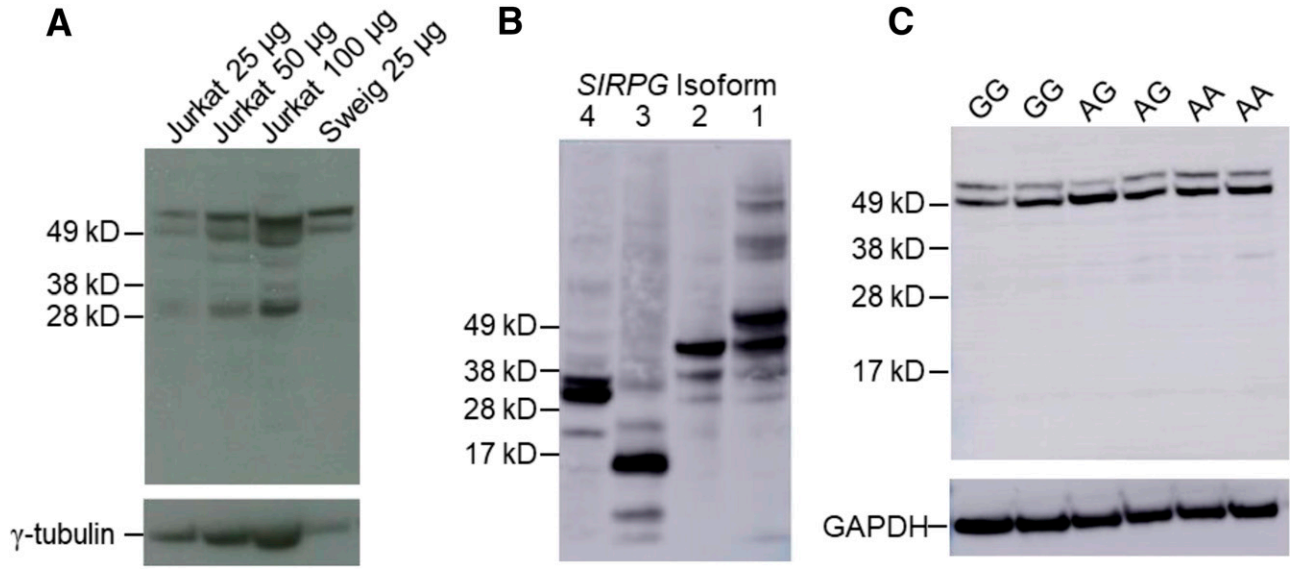

Figure 2—Expression of SIRPγ isoforms in T cells. *A*: Varying amounts of protein lysate from Jurkat T cells or Sweig, a B lymphoblastoid cell, were immunoblotted with anti-SIRPγ antibody. The blot was subsequently stripped and reprobed with an antibody directed against γ-tubulin as a control for loading. *B*: Expression plasmids for each *SIRPG* isoform with a C-terminal V5 epitope tag were transiently transfected into HEK293T cells and protein lysates were immunoblotted with an antibody against V5. *C*: Protein lysates prepared from activated $CD4^+$ T cells from donors with differing genotypes at rs6043409 were immunoblotted with the same anti-SIRPγ antibody used in *A*. The blot was subsequently stripped and reprobed with an antibody directed against GAPDH as a control for loading.

with monoallelic mutations in exon 4, some modest surface and intracellular expression of SIRPγ was detected (Fig. 3). These results were consistent when experiments were repeated with a different anti-SIRPγ antibody (Supplementary Fig. 5). Together with the immunoblotting results, these findings indicate that the majority of cell-surface SIRPγ is derived from transcript isoform 1.

Functional Consequences of Variation in SIRPγ Expression

We tested whether ablating SIRPγ cell-surface expression would affect cell-cell adhesion by measuring conjugate formation between CRISPR/Cas9-targeted Jurkat clones that express CD47 but not SIRPγ, and wild-type clones that express both CD47 and SIRPγ. Piccio et al. (3) previously applied this assay to a CD47-deficient Jurkat line to demonstrate the dependence of conjugate formation on CD47 expression. *SIRPG*-targeted clones consistently formed greater numbers of conjugates when paired with wild-type clones as compared with other targeted clones (Fig. 4*A*). Targeted clones also displayed significantly increased cell-surface expression of CD47 relative to wild-type clones (Fig. 4*B*).

RNA-seq analysis of five *SIRPG*-targeted clones identified a number of genes whose expression was increased or decreased relative to that in four wild-type Jurkat clones (Supplementary Fig. 7). Focusing on downregulated genes that might reflect reduced CD47 signaling in the absence of SIRPγ, we found that there was significant enrichment for TNF-related genes (corrected $P = 0.039$). Several genes reported to be upregulated by CD47 stimulation, such as *BAX*, *PMAIP1*, and *DDIT3*, were downregulated in *SIRPG*-targeted clones.

Since variation at rs6043409 affects the proportion of *SIRPG* transcripts that are spliced to different isoforms, genotypes should correlate with the cell-surface expression of SIRPγ. To test this, we measured the cell-surface expression of SIRPγ in $CD4^+$ and $CD8^+$ T cells from

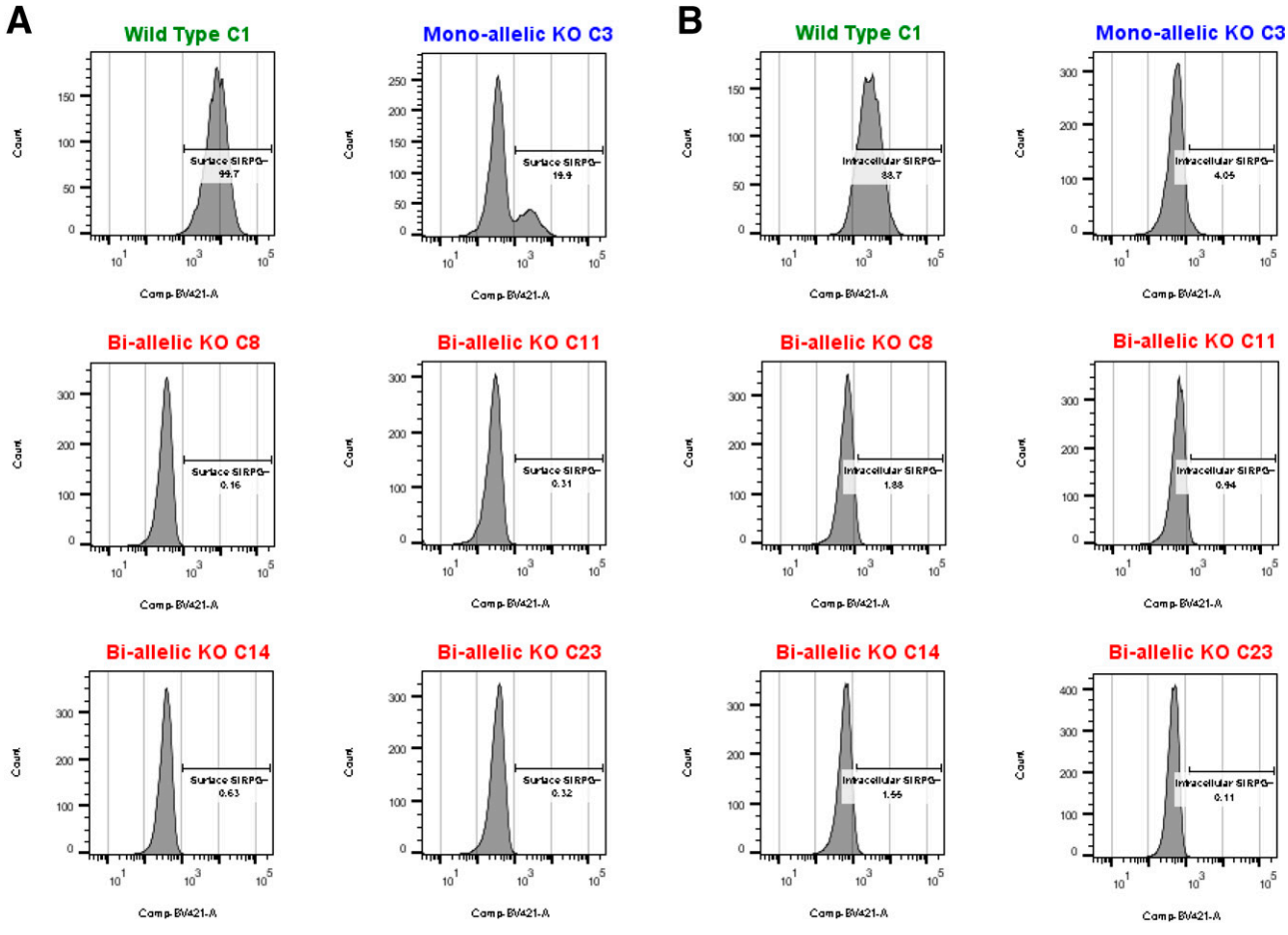

Figure 3—Cell-surface and intracellular expression of SIRPγ in Jurkat cells with CRISPR/Cas9-targeted mutations in exon 4 of *SIRPG*. Jurkat cell clones were acquired in a BD LSRFortessa and selected for no debris, morphology, singlets, and viability according to the gating strategy described in Supplementary Fig. 5. SIRPγ surface (*A*) and intracellular (*B*) expression levels were quantified in wild-type Jurkat p2 and clones carrying a SIRPγ mono- or biallelic truncating mutation (KO) in exon 4 with use of BV421 Mouse Anti-Human SIRPγ antibody.

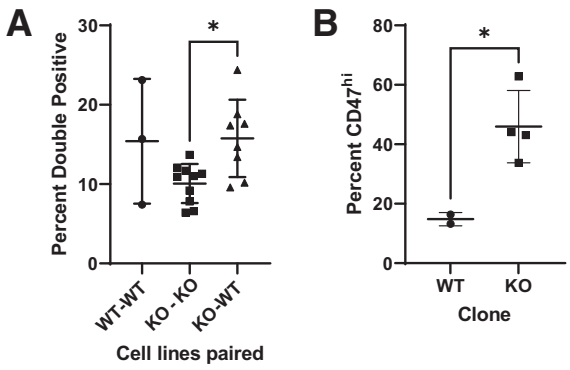

Figure 4—Doublet formation and CD47 cell-surface expression in *SIRPG*-targeted clones. *A*: Doublets were formed between individual pairs of Jurkat clones as indicated on the horizontal axis. The percentage of double-positive doublets formed was plotted. *B*: $CD47^{hi}$ surface expression levels were quantified as percentage of wild-type Jurkat p2 clones (WT) and clones carrying a SIRPγ biallelic truncating mutation in exon 4 (KO). $^{*}P < 0.05$.

healthy subjects representing each genotype at rs6043409. For both $CD4^{+}$ and $CD8^{+}$ T cells, the mean fluorescence intensity of SIRPγ differed significantly between subjects with different genotypes at rs6043409 (Fig. 5). The minor allele at rs6043409 (A) was associated with reduced expression of SIRPγ in a dose-dependent manner.

We examined the expansion of $CD4^{+}$ T cells derived from donors with different rs6043409 genotypes treated with bead-bound anti-CD3/CD28 and IL-2. Subjects with the GG genotype, who express higher levels of SIRPγ, showed a trend toward greater proliferation over the 11-day treatment period, but, overall, differences by genotype were not statistically significant (Supplementary Fig. 8).

DISCUSSION

Regulation of Gene Expression by Alternative Splicing

Alternative splicing is primarily considered a mechanism for creating protein diversity through the differential incorporation of structural or functional motifs in the products of a single gene (19,20). Less well appreciated is its potential for regulating gene expression posttranscriptionally by diverting transcripts derived from a single promoter to alternative isoforms, which may have varying ability to encode functional proteins. When coupled with genetic variants that affect the efficiency or specificity of the splicing process, an opportunity for posttranscriptional quantitative regulation of gene expression is created. We demonstrate here that such a mechanism acts on *SIRPG* and, specifically, that a credible causative genetic variant for type 1 diabetes, rs6043409, modulates cell-surface expression of SIRPγ by altering splicing efficiency with potential impacts on cell-cell adhesion and gene expression in T cells.

The functional domain of SIRPγ that binds CD47 is encoded entirely within exon 2 of *SIRPG*, which is present in all transcript isoforms studied here. Exons 3 and 4 can be used alternatively or eliminated. We observed that isoform 3, which lacks both exons 3 and 4, is readily detectable as a transcript; indeed, in subjects with type 1 diabetes homozygous for the minor allele at rs6043409, it is the predominant *SIRPG* transcript produced. Transcript isoform 3 can produce protein after transient transfection of HEK293T cells, but no corresponding protein is detectable in primary T cells by immunoblotting or cell-surface staining. Isoform 4 is transcribed at a relatively low level and does produce a small amount of endogenous protein detectable by immunoblotting. However, this protein is not detected on the cell surface where it could engage CD47.

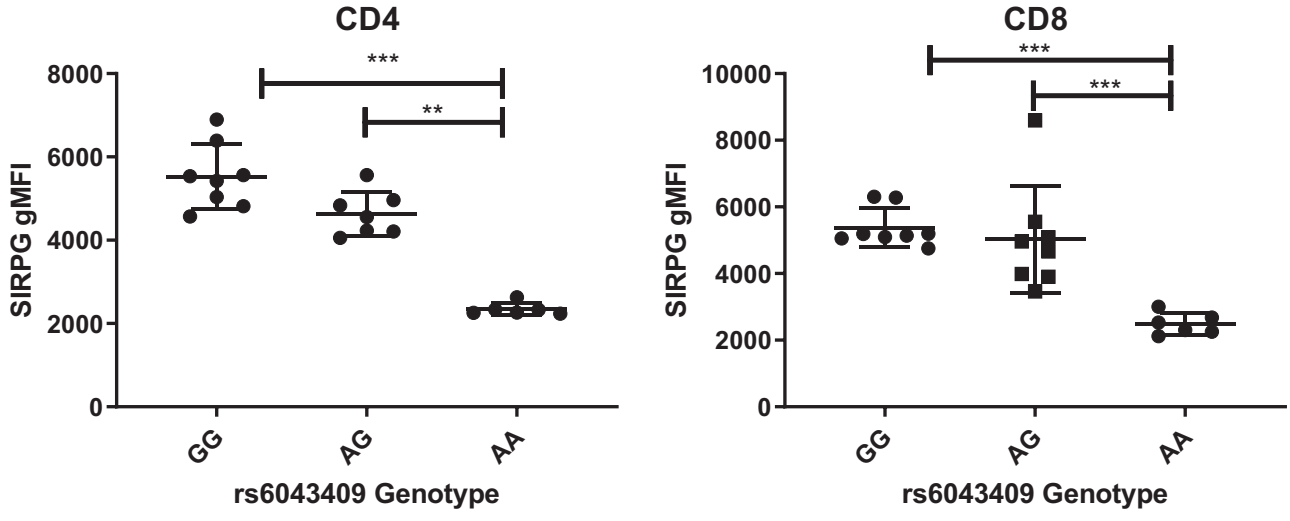

Figure 5—T cell surface expression of SIRPγ relative to rs6043409 genotype. Statistically significant differences in expression between genotype are indicated by $^{**}P < 0.01$ and $^{***}P < 0.001$. gMFI, geometric mean fluorescence intensity.

Like most membrane-bound proteins in the secretory pathway, SIRPγ is glycosylated. Four N-linked glycosylation sites have been reported in SIRPγ (21); all four sites are present in isoforms 1 and 2, none in isoform 3, and one site in isoform 4. N-linked glycosylation plays a significant role in quality control of protein folding in the endoplasmic reticulum as well as in stabilizing protein structure (22). One possible explanation for the failure to detect endogenous protein corresponding to transcript isoform 3 is that lack of glycosylation results in its turnover.

SIRPG and Risk for Type 1 Diabetes

The major allele at rs6043409 confers risk for type 1 diabetes and, in our study, is associated with higher cell-surface levels of SIRPγ on both $CD4^+$ and $CD8^+$ T cells. SIRPγ lacks discernable internal signaling motifs. Its interaction with PBMCs is mediated solely by CD47 (2,3), suggesting that binding to CD47 is key to its effects. CD47 is not implicated as a risk locus for type 1 diabetes. SIRPα, which is expressed on myeloid and neuronal cells, binds CD47 with an ∼10-fold greater affinity than SIRPγ (2). Thus, it likely is not the engagement of CD47 per se that confers risk for type 1 diabetes but, rather, its engagement by a ligand, SIRPγ, expressed on T cells. Indeed, SIRPγ expression provides the only opportunity for T cells to engage and signal through CD47. Using *SIRPG* CRISPR/Cas9-targeted Jurkat clones, we show here that SIRPγ increases cell-cell affinity and that in its absence, genes normally upregulated by CD47 engagement are expressed at lower levels.

SIRPγ-CD47 engagement has been reported to increase $CD4^+$ T cell proliferation in response to suboptimal concentrations of anti-CD3 (3). We observed a trend toward greater expansion of purified $CD4^+$ T cells from donors homozygous for the major allele at rs6043409 upon anti-CD3/CD28 stimulation. However, differences between genotypes were not statistically significant, suggesting that any effect of *SIRPG* genotype on proliferation is likely secondary to its effects on cell-cell adhesion or only apparent in the absence of CD28 signaling. Increased SIRPγ expression might also contribute to autoimmunity by signaling through CD47 expressed on nonlymphoid cell types. For example, engagement of CD47 on endothelial cells by SIRPγ is required for *trans*-endothelial migration of T cells (4). The increased expression of SIRPγ associated with the risk allele at rs6043409 might enhance this process, which, in the context of type 1 diabetes, could increase access of T cells to sites of ongoing inflammation such as the pancreas.

Unlike the majority of genetic variants associated with risk for type 1 diabetes, the major allele at rs6043409 is the risk allele. Our study indicates that this allele results in increased cell-surface expression of SIRPγ on T cells. This creates a potential therapeutic opportunity, as strategies that either reduce SIRPγ expression or block its access to ligand could potentially interfere with type 1 diabetes pathogenesis.

Funding. This work was supported by grants from the National Institute of Diabetes and Digestive and Kidney Diseases (NIDDK) (R01DK116954, R01DK106718) and Division of Intramural Research, National Institute of Allergy and Infectious Diseases (NIAID) (P01AI042288), National Institutes of Health. This research was performed using resources developed by the Type 1 Diabetes Genetics Consortium, a collaborative clinical study sponsored by the National Institute of Diabetes and Digestive and Kidney Diseases (NIDDK), National Institute of Allergy and Infectious Diseases (NIAID), National Human Genome Research Institute (NHGRI), National Institute of Child Health and Human Development (NICHD), and Juvenile Diabetes Research Foundation International (JDRF).

Duality of Interest. P.C. is a stockholder in Amgen, Inc. No other potential conflicts of interest relevant to this article were reported.

Author Contributions. M.J.S. carried out experiments, directed the study, and edited the manuscript. L.P. carried out the CRISPR/Cas9 experiments and edited the manuscript. J.R.B.N. carried out the RNA-seq analyses and edited the manuscript. P.C. oversaw the study and wrote and edited the manuscript. P.C. is the guarantor of this work and, as such, had full access to all the data in the study and takes responsibility for the integrity of the data and the accuracy of the data analysis.

References

1. Barclay AN, Van de Berg TK. The interaction between signal regulatory protein alpha (SIRPα) and CD47: structure, function, and therapeutic target. Annu Rev Immunol 2014;32:25–50

2. Brooke G, Holbrook JD, Brown MH, Barclay AN. Human lymphocytes interact directly with CD47 through a novel member of the signal regulatory protein (SIRP) family. J Immunol 2004;173:2562–2570

3. Piccio L, Vermi W, Boles KS, et al. Adhesion of human T cells to antigen-presenting cells through SIRPbeta2-CD47 interaction costimulates T-cell proliferation. Blood 2005;105:2421–2427

4. Stefanidakis M, Newton G, Lee WY, Parkos CA, Luscinskas FW. Endothelial CD47 interaction with SIRPgamma is required for human T-cell transendothelial migration under shear flow conditions in vitro. Blood 2008;112:1280–1289

5. Barrett JC, Clayton DG, Concannon P, et al.; Type 1 Diabetes Genetics Consortium. Genome-wide association study and meta-analysis find that over 40 loci affect risk of type 1 diabetes. Nat Genet 2009;41:703–707

6. Onengut-Gumuscu S, Chen WM, Burren O, et al.; Type 1 Diabetes Genetics Consortium. Fine mapping of type 1 diabetes susceptibility loci and evidence for colocalization of causal variants with lymphoid gene enhancers. Nat Genet 2015;47:381–386

7. Westra HJ, Martínez-Bonet M, Onengut-Gumuscu S, et al. Fine-mapping and functional studies highlight potential causal variants for rheumatoid arthritis and type 1 diabetes. Nat Genet 2018;50:1366–1374

8. Sinha S, Borcherding N, Renavikar PS, et al. An autoimmune disease risk SNP, rs2281808, in SIRPG is associated with reduced expression of SIRPγ and heightened effector state in human CD8 T-cells. Sci Rep 2018;8:15440

9. Newman JRB, Conesa A, Mika M, et al. Disease-specific biases in alternative splicing and tissue-specific dysregulation revealed by multitissue profiling of lymphocyte gene expression in type 1 diabetes. Genome Res 2017;27:1807–1815

10. Pfaffl MW. A new mathematical model for relative quantification in real-time RT-PCR. Nucleic Acids Res 2001;29:e45

11. Thierry-Mieg D, Thierry-Mieg J. AceView: a comprehensive cDNA-supported gene and transcripts annotation. Genome Biol 2006;7 Suppl 1 (Suppl. 1):S12.1–14
12. Li B, Dewey CN. RSEM: accurate transcript quantification from RNA-Seq data with or without a reference genome. BMC Bioinformatics 2011;12:323
13. Ng PC, Henikoff S. Predicting deleterious amino acid substitutions. Genome Res 2001;11:863–874
14. Adzhubei IA, Schmidt S, Peshkin L, et al. A method and server for predicting damaging missense mutations. Nat Methods 2010;7:248–249
15. Kelley LA, Mezulis S, Yates CM, Wass MN, Sternberg MJ. The Phyre2 web portal for protein modeling, prediction and analysis. Nat Protoc 2015;10:845–858
16. Cartegni L, Wang J, Zhu Z, Zhang MQ, Krainer AR. ESEfinder: a web resource to identify exonic splicing enhancers. Nucleic Acids Res 2003;31:3568–3571
17. Newman JRB, Concannon P, Tardaguila M, Conesa A, McIntyre LM. Event Analysis: using transcript events to improve estimates of abundance in RNA-seq data. G3 (Bethesda) 2018;8:2923–2940
18. Gioia L, Siddique A, Head SR, Salomon DR, Su AI. A genome-wide survey of mutations in the Jurkat cell line. BMC Genomics 2018;19:334
19. Nilsen TW, Graveley BR. Expansion of the eukaryotic proteome by alternative splicing. Nature 2010;463:457–463
20. Yang X, Coulombe-Huntington J, Kang S, et al. Widespread expansion of protein interaction capabilities by alternative splicing. Cell 2016; 164:805–817
21. Wollscheid B, Bausch-Fluck D, Henderson C, et al. Mass-spectrometric identification and relative quantification of N-linked cell surface glycoproteins. Nat Biotechnol 2009;27:378–386
22. Xu C, Ng DT. Glycosylation-directed quality control of protein folding. Nat Rev Mol Cell Biol 2015;16:742–752